Doping metal ions only onto the catalyst surface

Ji-Chuan Xu [a], Yan-Li Shi [a], Ji-Er Huang [a], Bo Wang [b], Hu-Lin Li [a,*]

[a] *Department of Chemistry, Lanzhou University, Lanzhou 730000, PR China*
[b] *State Key Laboratory of Solid Lubrication, Lanzhou Institute of Chemical Physics, Chinese Academy of Science,*
Lanzhou 730000, PR China

Abstract

A new method to dope Zn^{2+} ions only onto the surface of titanium dioxide is proposed here. The photocatalyst TiO_2(-Zn) exhibits higher photocatalytic activity than pure TiO_2 for the degradation of methyl orange in water. The activity increases when separate ZnO phase is removed via an acid treatment. The results of FT-IR, XRD, AAS and XPS analysis show that the Zn^{2+} ions are located on the surface of TiO_2 nanoparticles and bonded with oxygen atoms around it. The Zn^{2+} ions on the surface inhibit electron–hole pair recombination as a charge separation center.
© 2004 Elsevier B.V. All rights reserved.

Keywords: Titanium dioxide; Doping; Zinc ions; Surface

1. Introduction

Titanium dioxide has received a lot of attention as a promising material for photocatalysis [1], liquid solar cell [2] and degradation of pollutants [3]. The photocatalylic efficiency of TiO_2 depends partially upon the relative degree of branching of the reactive electron–hole pairs into interfacial charge-transfer reactions [4]. In order to enhance interfacial charge-transfer reactions, the catalyst has been modified by selective metal ion doping of the crystalline TiO_2 matrix [5–19]. For example, Fe^{3+}- and Ag^+-doped TiO_2 were shown to increase the efficiency of the oxidation of sucrose to carbon dioxide [14]; $Ti_{1-x}Zr_xO_2$ solid solution exhibited higher photocatalytic activity than pure anatase TiO_2 [16]; Mo^{5+}-doped TiO_2 enhanced photodecomposition of Rhodamine B [17]. The presence of metal ion dopants in the TiO_2 crystalline matrix significantly influences photoreactivity, charge carrier recombination rates and interfacial electron-transfer rates.

Generally, the transition metal-doped TiO_2 was prepared by adding metal salt into the TiO_2 colloid [5–19]. Choi et al.

[18,19] have prepared 21 metal ions-doped TiO_2 colloids using this method and conducted systematic studies on them. This method allowed the metal ions located both inside and outside the lattice. In this doping system, the charge trapped by metal ions in lattice needs to transfer to the interface to initiate the photoreaction, therefore, the charge release and migration in the lattice are equally important as well as the charge trapping.

Here, we report a new doping method, by which metal ions are doped on the TiO_2 surface rather than in the lattice. In this system, the transfer of charge trapped by metal ions from the inside of lattice to interface can be neglected because there is no metal ion doped in lattice. The metal ions (zinc ions) act as a charge separation center on the TiO_2 surface to enhance the photocatalytic activity. Surface-doped TiO_2 is prepared via a ligand exchange reaction between zinc acetylacetonate and hydroxide radicals on TiO_2 surface. The approach is also applicable to prepare other transition metals surface-doped TiO_2. This is not the first report on Zn-doped TiO_2 [19], but actually a yet-unreported method for preparing surface-doped TiO_2 to the best of the author's knowledge.

The photocatalytic activity of the new system for degradation of methyl orange was determined. The characterizations were also done using FT-IR, XRD, AAS and XPS.

* Corresponding author. Tel.: +86 109318912517;
fax: +86 9318912582.
E-mail address: lihl@lzu.edu.cn (H.-L. Li).

In addition, a photocatalytic mechanism of this new system was proposed here based on the experimental results and theoretical considerations.

2. Experimental

2.1. Synthesis of TiO$_2$ nanoparticles

A sample of tetrabutyl titanate (98%, Beijing Chemical Factory, Beijing, China) dissolved in absolute ethanol at a volume ratio 1:14 was added dropwise under vigorous stirring to a mix solution which contained acetic acid, absolute ethanol and distilled water at a volume ratio 3:10:10. The resulting transparent colloidal suspension was evaporated (35 °C) and dried under vacuum, and finally annealed at 500 °C for crystallization.

2.2. Synthesis of zinc acetylacetonate

Acetyl acetone (99%, Beijing Chemical Factory, Beijing, China) was added to the ethanol solution of Zn(Ac)$_2$ under stirring. The white product was produced after 8 h and separated from solution by filtration. After washing with ethanol and dried under vacuum, the pure Zn(acac)$_2$ was ready for next reaction.

2.3. Synthesis of TiO$_2$(-Zn) nanoparticles

TiO$_2$ nanopowders were added to an acetonitrile solution of Zn(acac)$_2$. After stirring for 6 h and aging for 24 h, this solution was centrifugalized and washed with distilled water to obtain the powdered product. The powdered product was dried under vacuum and annealed at 500 °C. As it cooled down naturally, it was treated with 1 M HCl aqueous solutions under stirring for 4 h. The acid treatment was repeated several times until the pH value of HCl solution had no change any more after treatment. The final product was washed with distilled water and dried under vacuum.

2.4. Characterization of TiO$_2$(-Zn) nanoparticles

The FT-IR analysis was carried out by a Nicolet AVATAR 360. X-ray diffraction patterns were recorded with a Rigaku Model D/max 2400 diffractometer using Cu Kα radiation. The elementary composition was determined by an atomic absorption spectrometer (AAS, WFX-10) using flame method. XPS measurements were performed in an X-ray photoelectron spectrometer PHI-5702 using the Al Kα X-ray beam. All the binding energies were referenced to the C$_{1s}$ peak at 284.8 eV.

2.5. Measurement of photocatalytic activity

Photocatalytic activity experiments of TiO$_2$(-Zn) nanoparticles for the degradation of methyl orange in water were performed in a light reactor. The catalysts were dispersed in a 20 mg/L methyl orange aqueous solution. The weight of the photocatalyst used in each experiment was kept at 0.2 g. The reactor was sparged with air at 0.2 m^3/h and illuminated by a 400 W high-pressure mercury lamp. The concentrations of methyl orange solution were quantified by a VIS-7220 spectrophotometer at 464 nm [20].

3. Results

3.1. Analysis of FT-IR results

The FT-IR spectra are shown in Fig. 1. The reaction between TiO$_2$ nanoparticles and Zn(acac)$_2$ resulted in the white powdered product. From its spectra, three peaks at 526 cm^{-1}, 1411 cm^{-1} and 1570 cm^{-1} can be observed. According to the standard spectra of acetyl acetone and TiO$_2$, two peaks should be attributed to the ligand acac, 1411 cm^{-1} for –CH$_3$ and 1570 cm^{-1} for a combined C–C and C–O stretching vibrations, and the other strong peak at 526 cm^{-1} should be attributed to Ti–O in TiO$_2$. After annealing, the two characteristic peaks of –acac disappear, and there is only a strong peak at 495 cm^{-1}. It indicates that the organic ligand was completely eliminated after annealing at 500 °C. At the same time, the metal oxide TiO$_2$(-Zn) was formed by thermolysis of the powdered product [21].

3.2. Analysis of XRD and AAS

The X-ray diffraction patterns of the metal oxide TiO$_2$(-Zn) and that with HCl solution treatment are shown in Fig. 2. XRD results show that the oxide TiO$_2$(-Zn) formed in annealing procedure is mainly in anatase phase, and some
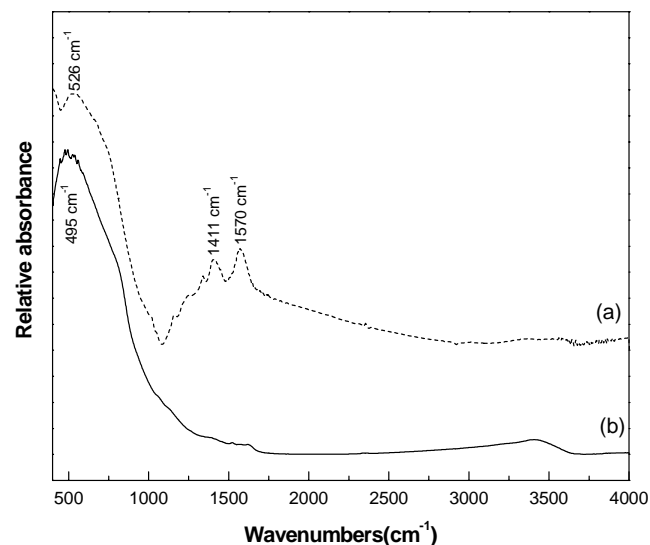

Fig. 1. FT-IR spectra of: (a) the product obtained from the reaction between TiO$_2$ and Zn(acac)$_2$ and (b) the metal oxide obtained after annealing.
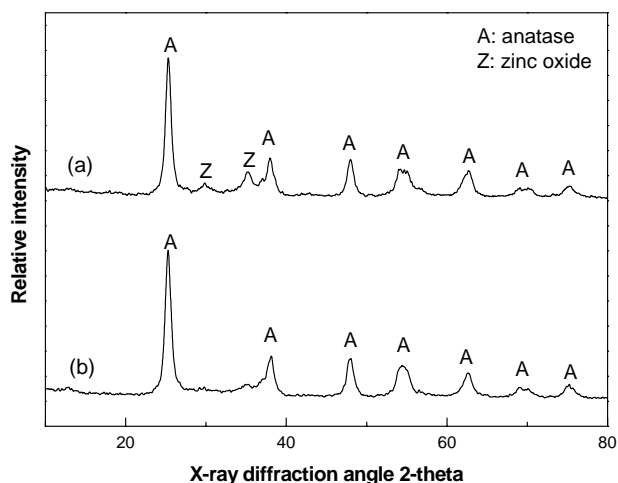
Fig. 2. XRD patterns of: (a) the metal oxide TiO_2(-Zn) and (b) that with HCl treatment.

ZnO is also present in TiO_2(-Zn) powder. To remove these ZnO, the TiO_2(-Zn) powder was treated with HCl solution. The XRD pattern of TiO_2(-Zn) with HCl treatment shows that the final product is in pure anatase phase and there is no separate ZnO phase or other phase in it. The result of AAS analysis shows that 0.75 mol% Zn of TiO_2 is still found in the final product. Therefore, we can exclude the possibility of Zn^{2+} substituting the lattice position of Ti^{4+} in TiO_2 crystalline; otherwise the XRD peaks for anatase would be shifted to some extent [22]. It can be inferred from the results of XRD and AAS that Zn^{2+} ions in pure TiO_2(-Zn) (without separate ZnO) should be located on the surface of TiO_2 particles.

3.3. Results of XPS measurements

According to XPS measurement on the final product (Fig. 3), a binding energy of $Zn_{2p3/2}$ is observed at 1021.17 eV, which is typical of Zn^{2+} that bonds with oxygen atoms. The binding energies for $Ti_{2p3/2}$ and $Ti_{2p1/2}$ are at 485.3 eV and 464.0 eV, respectively. These values are consistent with those reported for titanium in TiO_2. Based on the peak area ratio, there is about 5.65 mol% Zn of TiO_2 in the final product, which was much larger than the result of AAS analysis. Because the XPS result corresponds to the surface composition, while AAS result gives the average composition of the sample, it can be concluded that Zn^{2+} ions are primarily located on the TiO_2 surface. The XPS results lead to the conclusion that the dopant zinc presents as Zn^{2+} on the surface of TiO_2 and bonds with oxygen atoms.

3.4. Photocatalytic activity for degradation of methyl orange in water

The percent of residual methyl orange at different stages over pure TiO_2, the metal oxide TiO_2(-Zn) and the final
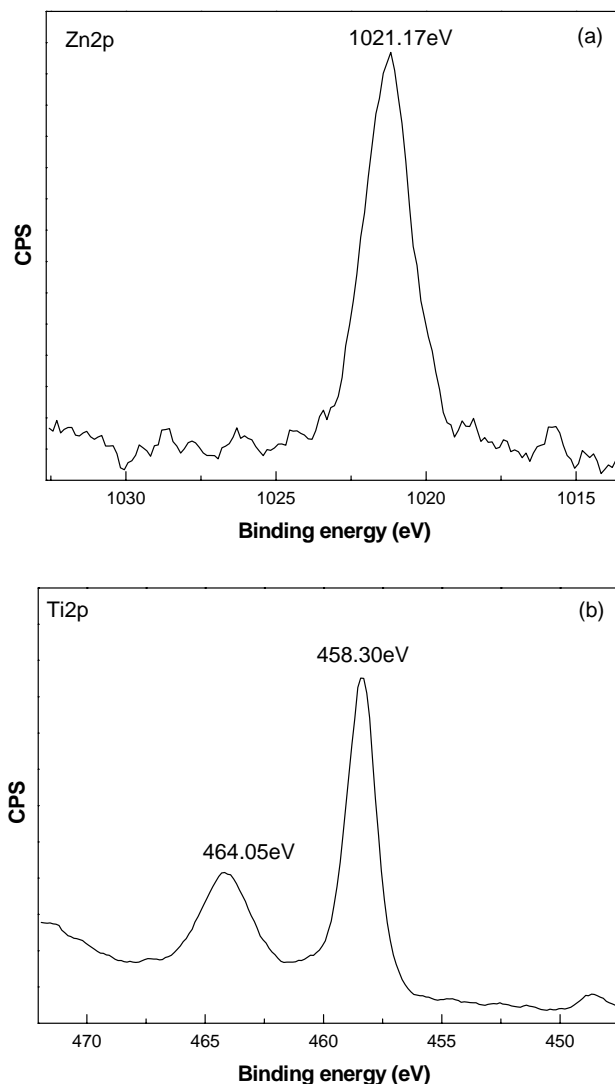

Fig. 3. XPS spectrum of: (a) Zn_{2p} and (b) Ti_{2p} in final product.

product under UV light irradiation are shown in Fig. 4. For pure TiO_2, the residual methyl orange are 0.859, 0.748 and 0.685 corresponding to irradiation time 1 h, 2 h and 3 h. For final product, there remain 0.742, 0.542 and 0.403 methyl orange after irradiated for 1 h, 2 h and 3 h. The final product (pure TiO_2(-Zn)) had highest activity among the three catalysts. The metal oxide TiO_2(-Zn) without HCl treating showed lower activity than pure TiO_2(-Zn) did, and the residual methyl orange are 0.799, 0.637 and 0.528 for the same irradiation time.

4. Discussion

4.1. Synthesis process of TiO_2(-Zn)

TiO_2 nanoparticles have a large number of dangling bonds –OH on its surface and these dangling bonds have high reactivity [4]. On the other hand, the ligands of $Zn(acac)_2$ have
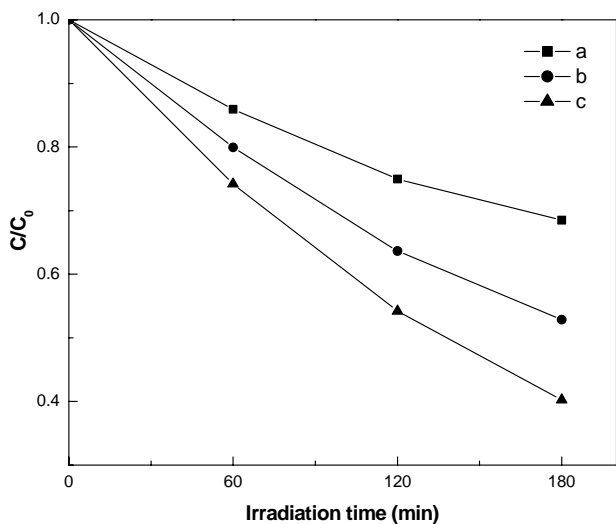
Fig. 4. The residual methyl orange at different irradiation time for: (a) pure TiO$_2$, (b) the metal oxide TiO$_2$(-Zn) and (c) the final product (pure TiO$_2$(-Zn)).

protophilia which can make the proton in –OH more active [21]. Therefore, it is possible that ligand exchange takes place between the dangling bongs and ligands of Zn(acac)$_2$. The exchange reaction is proposed as follows:

$$Zn(acac)_2 + Ti–OH \rightarrow Zn(acac)(–O–Ti) + Hacac \qquad (1)$$

According to the results of FT-IR analysis, the reaction product between TiO$_2$ and Zn(acac)$_2$ is the precursor of the oxide TiO$_2$(-Zn). When annealed at 500 °C, the precursor takes a thermal decomposition and the organic ligands are burnt away. The oxide TiO$_2$(-Zn) formed in annealing procedure consists of pure anatase TiO$_2$(-Zn) and separate ZnO. The separate ZnO we find in XRD patterns is the resultant of thermolysis of the Zn(acac)$_2$ adsorbed on TiO$_2$ by physisorption. Since the separate ZnO is removed, according to the results of XRD, AAS and XPS, it can be concluded that Zn^{2+} ions in pure TiO$_2$(-Zn) are primarily located on the surface of TiO$_2$ nanoparticles and bonded with oxygen atoms around them. The brief synthesis process of TiO$_2$(-Zn) is illustrated by Fig. 5.

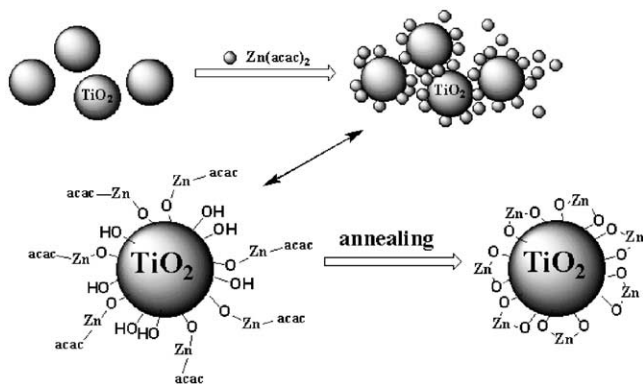Fig. 5. The synthesis process of TiO$_2$(-Zn) catalyst.

4.2. The photocatalytic mechanism

The results of degradation experiments shows that both TiO$_2$(-Zn) with and without HCl treatment have higher photoactivities than pure TiO$_2$ for the degradation of methyl orange. That should be ascribed to the doping of Zn^{2+}, the foreign metal ions, in the surface of TiO$_2$ because the foreign metal ions are helpful for inhibiting electron–hole pair recombination [4,23,24] and enhancing interfacial charge transfer reactions [18]. It can be seen that the photoactivity of TiO$_2$(-Zn) was increased when treated with HCl solution. The reason for that is primarily because the excess ZnO in TiO$_2$(-Zn) shield the photocatalyst from UV light. When the excess ZnO is removed, the photoactivity is enhanced. Additionally, the acid treatment promotes the surface acidity, which also increases the photocatalytic activity of TiO$_2$ [25–27]. Based on experimental results, we propose that the photocatalytic reactions of TiO$_2$(-Zn) nanoparticles take place by the following mechanism:

$$TiO_2 + h\nu \rightarrow e^- + h^+ \qquad (2)$$

$$Ti^{4+} + e^- \rightarrow Ti^{3+} \qquad (3)$$

$$Zn^{2+} + e^- \rightarrow Zn^+ \qquad (4)$$

$$>OH^- + h^+ \rightarrow >OH^\bullet \qquad (5)$$

$$e^- (or\ Ti^{3+},\ Zn^+) + O \rightarrow O^- \qquad (6)$$

$$h^+ (or >OH^\bullet,) + R \rightarrow R^+ \qquad (7)$$

where O is an electron acceptor (oxidant) and R is an electron donor (reductant). Choi et al. [18] suggested that the charge release and migration in the lattice should not be neglected and was equally important as well as the charge trapping because the trapped charges need to be transferred to the interface to initiate the photoreactions. In this TiO$_2$(-Zn) system, the dopant Zn^{2+} ions are located on the surface of catalyst rather than in TiO$_2$ lattice, therefore, the charge release and migration in the lattice can be neglected for the charge trapped by Zn^{2+} in the TiO$_2$(-Zn) system. The Zn^{2+} ions on the surface of catalyst enhance the charge trapping and inhibit the e$^-$/h$^+$ pair recombination as a charge separation center. It should be noticed that the hole trapping of Zn^{2+} after the photoexcitation is less efficient than the electron trapping of Zn^{2+}, because it is difficult for $Zn^{2+}_{3d^{10}(^1s_0)}$ to lose a more electron. However, the Zn^{2+} ions enhance the photoactivity by trapping electron that enhance the separation of photogenerated electrons and holes, leaving holes available for oxidation of organic molecules.

5. Conclusion

TiO$_2$ nanoparticles doped with Zn^{2+} on its surface can be successfully prepared via a ligand exchange reaction and a further thermal treatment. The nanoparticles exhibit higher

photocatalytic activity than pure TiO_2 for the degradation of methyl orange in water. The increase in activity is due to the decrease of the e^-/h^+ pair recombination rate caused by Zn^{2+} ions on the surface of TiO_2.

Acknowledgements

References

[1] A.L. Linsebigler, G. Lu, J.T. Yates, Chem. Rev. 95 (1995) 735.
[2] B. O'Regan, M. Gratzel, Nature 353 (1991) 737.
[3] M.A. Fox, M.T. Dulary, Chem. Rev. 93 (1993) 341.
[4] M.R. Hoffmann, S.T. Martin, W. Choi, D.W. Bahnemann, Chem. Rev. 95 (1995) 69.
[5] D.W. Bahnemann, J. Monig, R. Chapmann, J. Phys. Chem. 91 (1987) 3782.
[6] J.A. Navio, F.J. Marchena, M. Roncel, M.A. Del la Rosa, J. Photochem. Photobiol. A: Chem. 55 (1991) 319.
[7] M. Gratzel, R.F. Howe, J. Phys. Chem. 94 (1990) 2566.
[8] J. Moser, M. Gratzel, R. Gallay, Helv. Chim. Acta 70 (1987) 1596.
[9] R.I. Bickley, J.S. Lees, R.J.D. Tilley, L. Palmisano, M. Schiavello, J. Chem. Soc., Faraday Trans. 88 (1992) 377.
[10] A. Sclafani, L. Palmisano, M. Schiavello, Res. Chem. Intermed. 18 (1992) 211.
[11] J. Kiwi, C. Morrison, J. Phys. Chem. 88 (1984) 6146.
[12] J. Kiwi, M. Gratzel, J. Phys. Chem. 90 (1986) 637.
[13] J. Sabate, M.A. Anderson, H. Kikkawa, Q. Xu, S. Cerveramarch, C.G. Hill Jr., J. Catal. 134 (1992) 36.
[14] V. Vamathevan, H. Tse, R. Amal, G. Low, S. McEvoy, Catal. Today 68 (2001) 201.
[15] V. Brezova, A. Blazkova, E. Borosova, M. Ceppan, R. Fiala, J. Mol. Catal. A: Chem. 98 (1995) 109.
[16] J.C. Yu, J. Lin, R.W.M. Kwok, J. Phys. Chem. B 102 (1998) 5094.
[17] K. Wilke, H.D. Breuer, J. Photochem. Photobiol. A: Chem. 121 (1999) 49.
[18] W. Choi, A. Termin, M.R. Hoffmann, J. Phys. Chem. 98 (1994) 13669.
[19] W. Choi, A. Termin, M.R. Hoffmann, Angew. Chem. Int. Ed. Engl. 33 (1994) 1091.
[20] C.J.G. Cornu, A.J. Colussi, M.R. Hoffmann, J. Phys. Chem. B 107 (2003) 3156.
[21] R. Molina, G. Poncelet, J. Phys. Chem. B 103 (1999) 11290.
[22] Z.S. Wang, C.H. Huang, Y.Y. Huang, Y.J. Hou, P.H. Xie, B.W. Zhang, H.M. Cheng, Chem. Mater. 13 (2001) 678.
[23] S.T. Martin, H. Herrmann, W. Choi, M.R. Hoffmann, Trans. Faraday Soc. 90 (1994) 3315.
[24] S.T. Martin, H. Herrmann, W. Choi, M.R. Hoffmann, Trans. Faraday Soc. 90 (1994) 3323.
[25] X. Fu, L.A. Clark, Q. Yang, M.A. Anderson, Environ. Sci. Technol. 30 (1996) 647.
[26] J. Papp, S. Soled, K. Dwight, A. Wold, Chem. Mater. 6 (1994) 496.
[27] C. Anderson, A.J. Bard, J. Phys. Chem. B 101 (1997) 2611.